Electronic Supplementary Information

Boosting electrocatalytic hydrogen evolution over Mo_2C-W_2C heterostructure by interface-induced electron modulation

Lijuan Jiang, Ruijing Wang, Huimin Zhou, Guang-Feng Wei*, Xuefeng Wang*

Shanghai Key Lab of Chemical Assessment and Sustainability, School of Chemical Science and Engineering, Tongji University, Shanghai, 200092, P. R. China.

*Corresponding Authors: weigf@tongji.edu.cn; xfwang@tongji.edu.cn

Contents

Table S1. Composition of samples obtained at different Mo/W feeding ratios.

products	$(NH_4)_6Mo_7O_{24}\cdot 4H_2O$[a] (g)	$(NH4)_6H_2W_{12}O_{40}\cdot xH_2O$[b] (g)	Mo/W[c]	Mo/(Mo+W)[d]
Mo_2C-W_2C/RGO-0.24	0.18	0.74	0.33	0.24
Mo_2C-W_2C/RGO-0.56	0.36	0.50	0.5	0.56
Mo_2C-W_2C/RGO-0.75	0.53	0.25	3.0	0.75

[a] Data was the molar amount of $(NH_4)_6Mo_7O_{24}\cdot 4H_2O$ used in synthesis. [b] Data was the molar amount of $(NH_4)_6H_2W_{12}O_{40}\cdot xH_2O$ used in synthesis. [c] Data was Mo/W feeding molar ratio. [d] Data was calculated from the result of EDS.

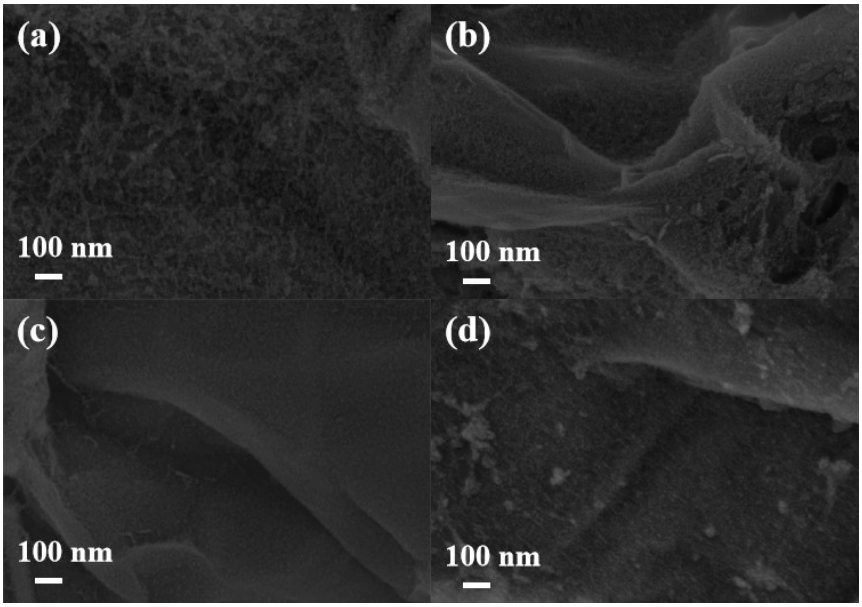

Fig. S1 SEM images of (a) Mo_2C/RGO, (b) Mo_2C-W_2C/RGO-0.75, (c) Mo_2C-W_2C/RGO-0.24, and (d) W_2C/RGO.

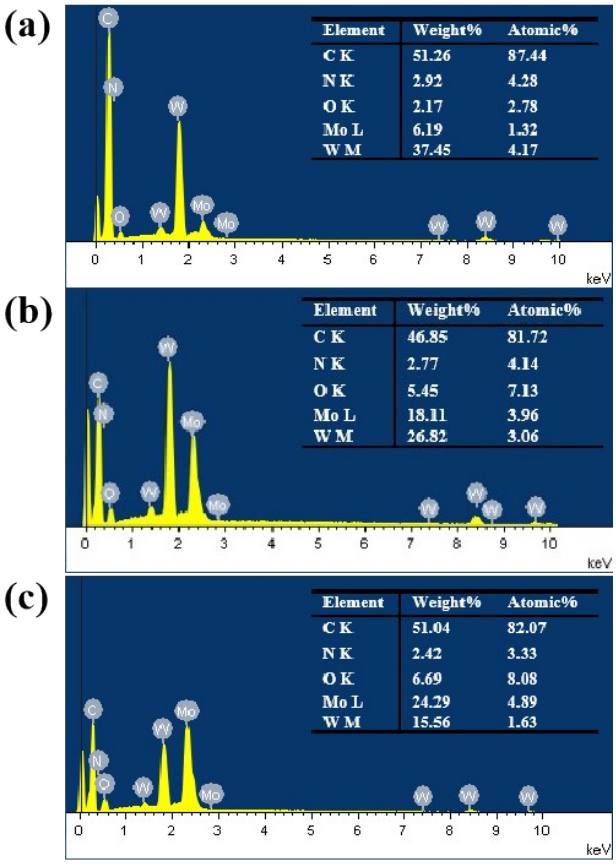

Fig. S2 EDS spectra of (a) Mo_2C-W_2C/RGO-0.24, (b) Mo_2C-W_2C/RGO-0.56, and (c) Mo_2C-W_2C/RGO-0.75.

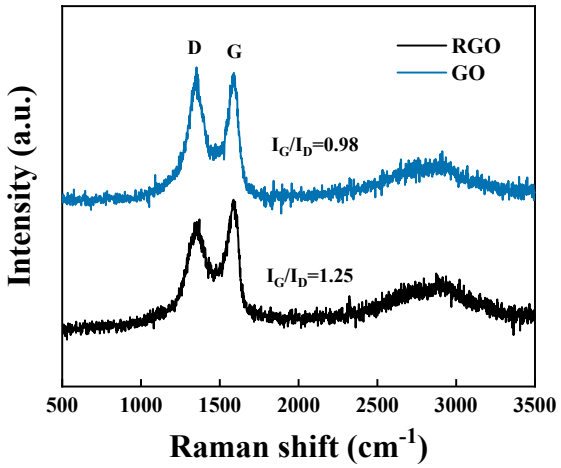

Fig. S3 Raman spectra of the GO and RGO.

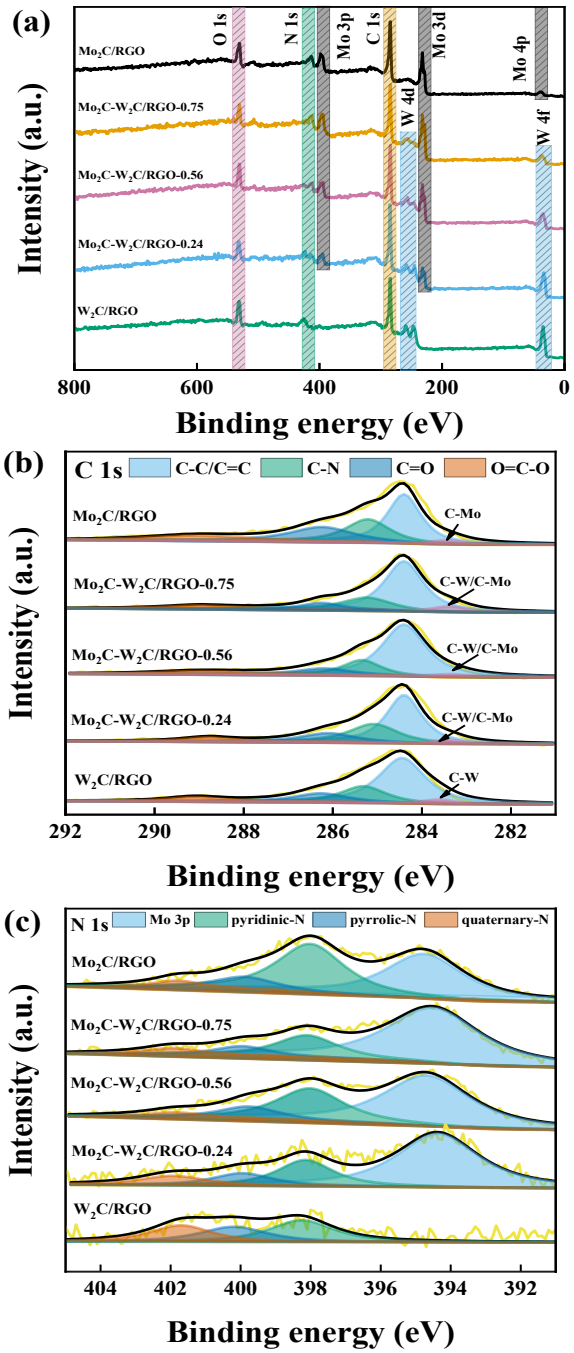

Fig. S4 (a) Survey XPS spectra. High-resolution XPS profiles of (b) C 1s; (c) N 1s.

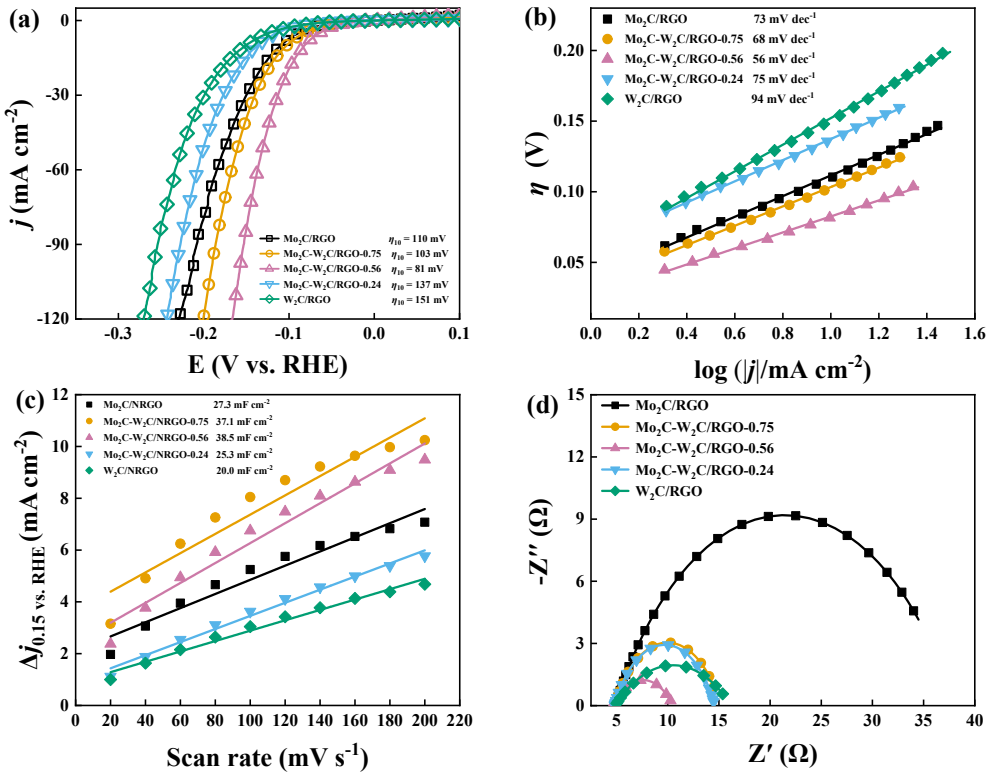

Fig. S5 (a) Polarization curves and (b) Tafel plots of Mo_2C/RGO, Mo_2C-W_2C/RGO-0.24, Mo_2C-W_2C/RGO-0.56, Mo_2C-W_2C/RGO-0.75, and W_2C/RGO in 0.5 M H_2SO_4. (c) The C_{dl} of different materials obtained at 0.15 V versus RHE. (d) Nyquist plots (at η = 200 mV).

Table S2. Comparison of catalytic parameters of Mo_2C/RGO, Mo_2C-W_2C/RGO-0.75, Mo_2C-W_2C/RGO-0.56, Mo_2C-W_2C/RGO-0.24, and W_2C/NRGO catalysts in 0.5 M H_2SO_4.

Catalysts	Onset potential (mV vs RHE)	η_{10} (mV vs RHE)	j_0 (mA cm^{-2})	Tafel slope (mV dec^{-1})	C_{dl} (mF dec^{-1})	R_{ct} (Ω)
Mo_2C/RGO	43	110	0.384	73	27.3	11.3
Mo_2C-W_2C/RGO-0.75	41	103	0.407	68	37.1	9.8
Mo_2C-W_2C/RGO-0.56	30	81	0.428	56	38.5	5.9
Mo_2C-W_2C/RGO-0.24	66	137	0.251	75	25.3	10.34
W_2C/NRGO	67	151	0.244	94	20.0	33.1

Table S3. Comparison of HER performance for Mo_2C-W_2C/RGO with other reported carbon-based electrocatalysts.

Catalyst	Electrolyte	Tafel slope (mV dec^{-1})	η_{10} (mV vs. RHE)	Ref.
Mo_2C-W_2C/RGO-0.56	**0.5 M H_2SO_4**	**56**	**81**	**This work**
	1.0 M KOH	**59**	**87**	
Twinned WCN	1.0 M KOH	-	138	1
	0.5 M H_2SO_4	65	128	
W_2C/WP@NC	1.0 M KOH	59.07	196.2	2
	0.5 M H_2SO_4	77.4	116.37	
W_2C@CNT-S8	1.0 M KOH	56.2	148	3
	0.5 M H_2SO_4	57.4	176	
Mo_2C@BNC	1.0 M KOH	57.4	145	4
	0.5 M H_2SO_4	68.3	184	
WC@C/NF	1.0 M KOH	94.7	124	5
	0.5 M H_2SO_4	-	208	
CoO/Mo_2C	1.0 M KOH	80	107	6
Co/Mo_2C@C	1.0 M KOH	68	98	7
Mo_2N-Mo_2C/HGr	1.0 M KOH	68	154	8
	0.5 M H_2SO_4	55	157	
Mo_2C/MoS_2-rGO	1.0 M KOH	52	112	9
WC-W_2C/HCDs	1.0 M KOH	72.2	116	10
	0.5 M H_2SO_4	52.5	96	
Mo_2C-CoO@N-CNFs-8	1.0 M KOH	76	115	11
Ni-W_2C	1.0 M KOH	73.8	88	12
WS_2/W_2C@NSPC	1.0 M KOH	72	205	13
	0.5 M H_2SO_4	68	126	
W-W_2C/CNT-6	1.0 M KOH	51	147	14
	0.5 M H_2SO_4	56	155	

Table S4. Comparison of catalytic parameters of different HER catalysts in 0.5 M H_2SO_4.

Catalyst	Onset potential (mV vs RHE)	η_{10} (mV vs RHE)	j_0 (mA cm^{-2})	Tafel slope (mV dec^{-1})	R_{ct} (Ω)
Pt/C	0	21	0.945	21	/
Mo_2C-W_2C/RGO-0.56	30	81	0.428	56	5.9
Mo_2C/RGO	43	110	0.384	73	11.3
W_2C/RGO	67	151	0.278	94	33.1
RGO	278	380	0.005	104	4040

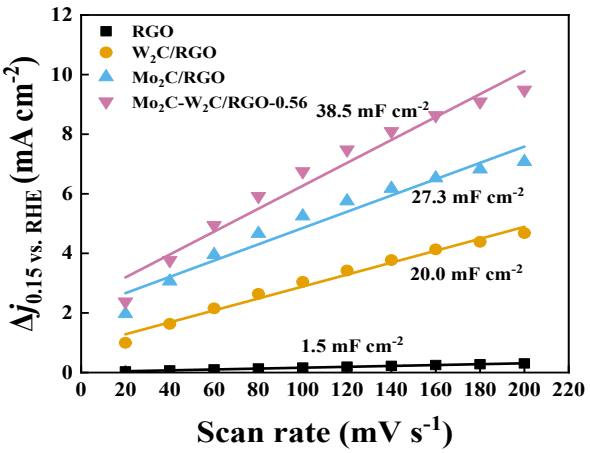

Fig. S6 The C_{dl} of different materials obtained at 0.15 V versus RHE in 0.5 M H_2SO_4.

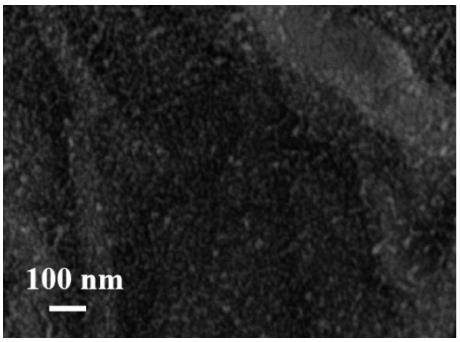

Fig. S7 SEM image of Mo_2C-W_2C/RGO-0.56 after long-term durability test in 0.5 M H_2SO_4.

Table S5. Comparison of catalytic parameters of different HER catalysts in 1.0 M KOH.

Catalyst	Onset potential (mV vs RHE)	η_{10} (mV vs RHE)	j_0 (mA cm^{-2})	Tafel slope (mV dec^{-1})	R_{ct} (Ω)
Pt/C	8	27	0.933	41	/
Mo_2C-W_2C/RGO-0.56	33	87	0.398	59	4.4
Mo_2C/RGO	66	134	0.120	64	6.5
W_2C/RGO	76	159	0.102	93	27.9
RGO	296	491	0.0316	189	279.7

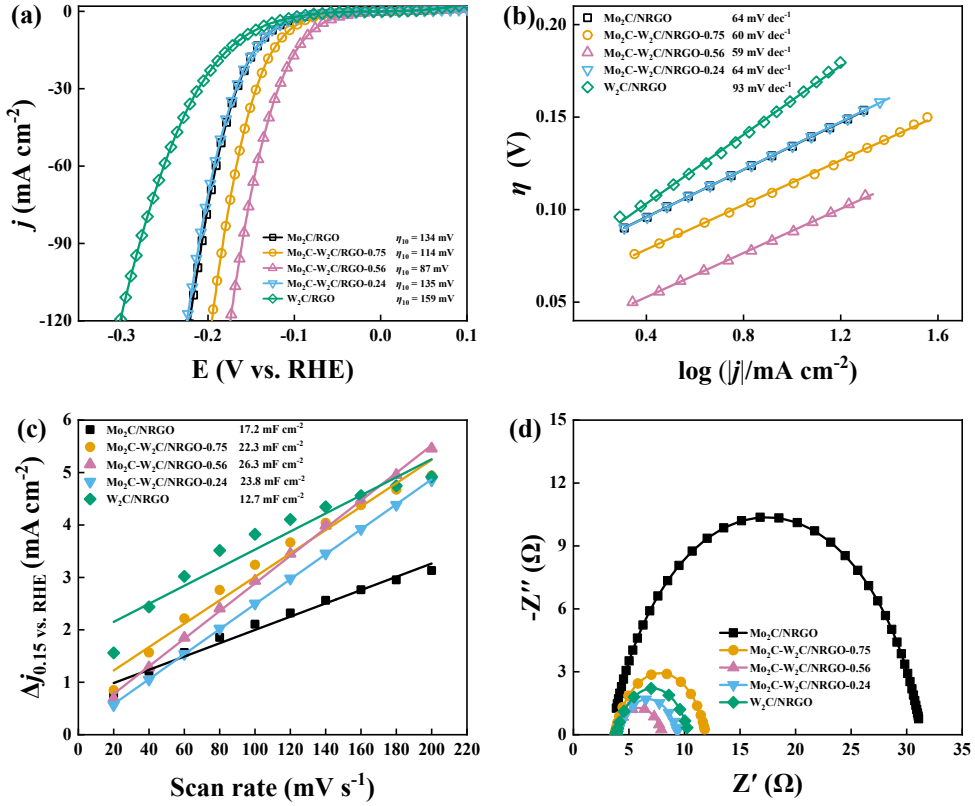

Fig. S8 (a) Polarization curves and (b) Tafel plots of Mo_2C/RGO, Mo_2C-W_2C/RGO-0.24, Mo_2C-W_2C/RGO-0.56, Mo_2C-W_2C/RGO-0.75, and W_2C/RGO in 1.0 M KOH. (c) The C_{dl} of different materials obtained at 0.15 V versus RHE. (d) Nyquist plots (at η = 200 mV).

Table S6. Comparison of catalytic parameters of Mo_2C/RGO, Mo_2C-W_2C/RGO-0.75, Mo_2C-W_2C/RGO-0.56, Mo_2C-W_2C/RGO-0.24, and W_2C/NRGO catalysts in 1.0 M KOH.

Catalysts	Onset potential (mV vs RHE)	η_{10} (mV vs RHE)	j_0 (mA cm^{-2})	Tafel slope (mV dec^{-1})	C_{dl} (mF dec^{-1})	R_{ct} (Ω)
Mo_2C/RGO	66	134	0.112	64	17.2	6.5
Mo_2C-W_2C/RGO-0.75	56	114	0.184	60	22.3	5.5
Mo_2C-W_2C/RGO-0.56	33	87	0.398	59	26.3	4.4
Mo_2C-W_2C/RGO-0.24	69	135	0.132	64	23.8	8.2
W_2C/NRGO	76	159	0.102	93	12.7	27.9

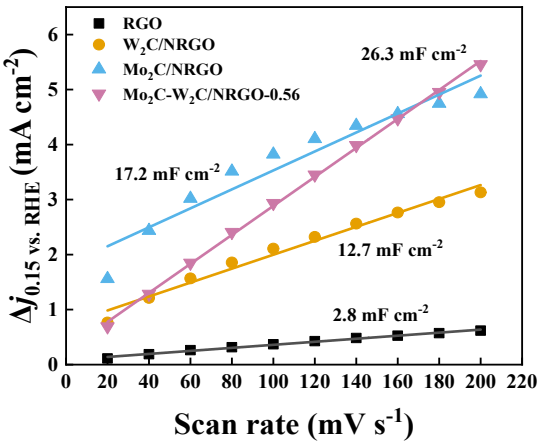

Fig. S9 The C_{dl} of different materials obtained at 0.15 V versus RHE in 1.0 M KOH.

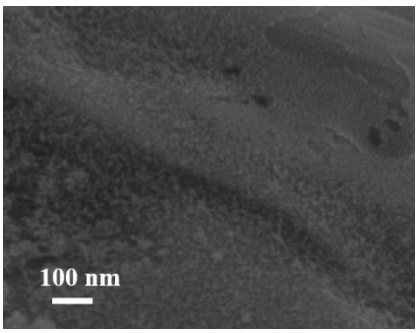

Fig. S10 SEM image of Mo_2C-W_2C/RGO-0.56 after long-term durability test in 1.0 M KOH.

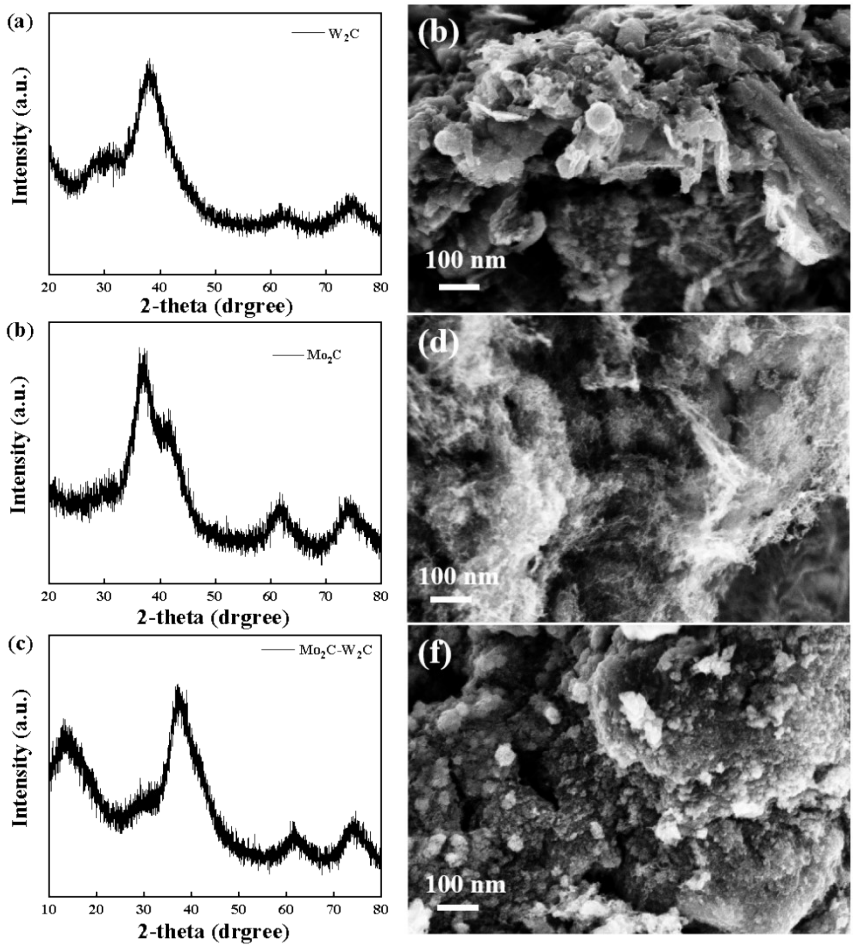

Fig. S11 (a) XRD pattern and (b) SEM image of W_2C. (c) XRD pattern and (d) SEM image of Mo_2C. (e) XRD pattern and (f) SEM image of Mo_2C-W_2C.

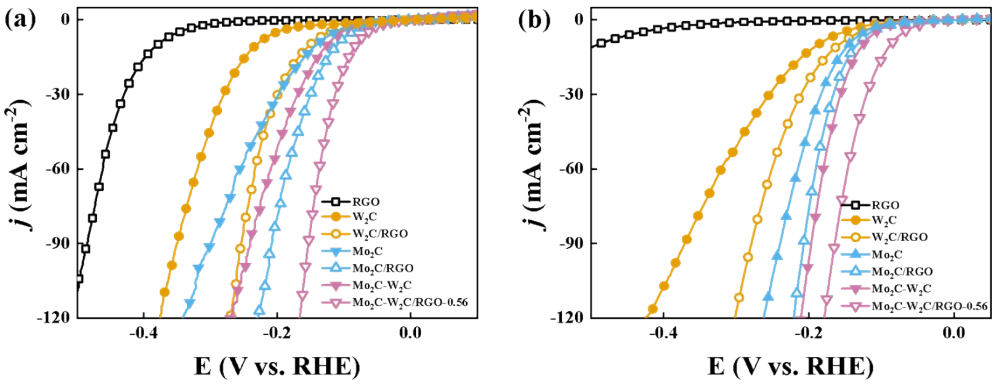

Fig. S12 (a) Polarization curves of RGO, W_2C, W_2C/RGO, Mo_2C, Mo_2C/RGO Mo_2C-W_2C, and Mo_2C-W_2C/RGO-0.56 in 0.5 M H_2SO_4. (b) Polarization curves of RGO, W_2C, W_2C/RGO, Mo_2C, Mo_2C/RGO Mo_2C-W_2C, and Mo_2C-W_2C/RGO-0.56 in 1.0 M KOH.

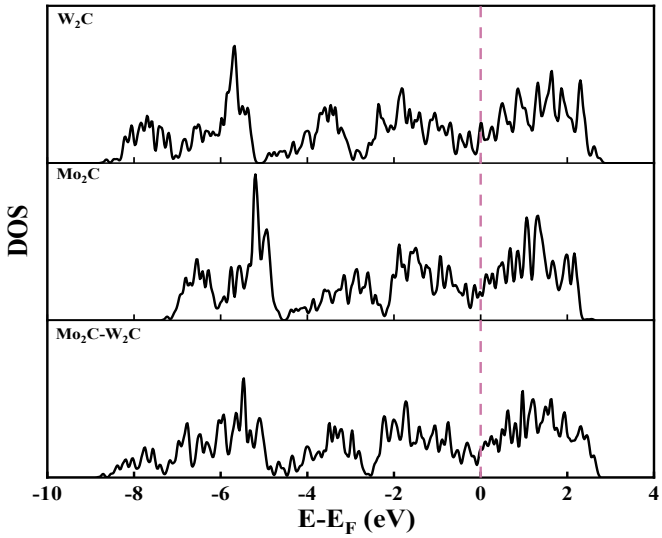

Fig. S13 The density of states for Mo_2C, W_2C, Mo_2C-W_2C. The dashed line denotes the position of the Fermi level.

REFERENCES

(1) Z. Kou, T. Wang, H. Wu, L. Zheng, S. Mu, Z. Pan, Z. Lyu, W. Zang, S. J. Pennycook, J. Wang. Twinned Tungsten Carbonitride Nanocrystals Boost Hydrogen Evolution Activity and Stability. Small, 2019, 15, 1900248.

(2) P. Wei, X. Sun, M. Wang, J. Xu, Z. He, X. Li, F. Cheng, Y. Xu, Q. Li, J. Han, H. Yang, Y. Huang. Construction of an N-Decorated Carbon-Encapsulated W_2C/WP Heterostructure as an Efficient Electrocatalyst for Hydrogen Evolution in Both Alkaline and Acidic Media. ACS Appl. Mater. Interfaces, 2021, 13, 53955-53964.

(3) Y. Hu, B. Yu, W. Li, M. Ramadoss, Y. Chen. W_2C nanodot-decorated CNT networks as a highly efficient and stable electrocatalyst for hydrogen evolution in acidic and alkaline media. Nanoscale, 2019, 11, 4876-4884.

(4) S. Wu, M. Chen, W. Wang, J. Zhou, X. Tang, D. Zhou, C. Liu. Molybdenum carbide nanoparticles assembling in diverse heteroatoms doped carbon matrix as efficient hydrogen evolution electrocatalysts in acidic and alkaline medium. Carbon, 2021, 171, 385-394.

(5) C. Tyagi, C. Lagrost, V. Dorcet, F. Tessier, B. Fabre. Carbon-Embedded Tungsten Carbide Electrocatalysts Derived from Self-Deposited Tungsten Oxide for the pH-Universal Hydrogen Evolution Reaction. ACS Appl. Energy Mater., 2023, 6, 6842-6850.

(6) H.-Y. Chen, L. Yang, R.-X. Wang, W.-J. Zhang, R. Liu, Y.-Z. Yun, N. Wang, S. Ramakrishna, L. Jiao, Y.-Z. Long. Constructing CoO/Mo_2C Heterostructures with Interfacial Electron Redistribution Induced by Work Functions for Boosting Overall

Water Splitting. Small, 2023, 2304086.

(7) S. Yuan, M. Xia, Z. Liu, K. Wang, L. Xiang, G. Huang, J. Zhang, N. Li. Dual synergistic effects between Co and Mo_2C in Co/Mo_2C heterostructurefor electrocatalytic overall water splitting. Chem. Eng. J., 2022, 430, 132697.

(8) H. Yan, Y. Xie, Y. Jiao, A. Wu, C. Tian, X. Zhang, L. Wang, H. Fu. Holey reduced graphene oxide coupled with an Mo_2N-Mo_2C heterojunction for efficient hydrogen evolution. Adv. Mater., 2018, 30, 1704156.

(9) X. Xu, H. Ma, W. Xu, X. Liu, H. Chu, L. Zhang, X. Wu. Heterostructure and phase engineering synergistically activated highly efficient alkaline hydrogen evolution in Mo_2C/MoS_2-rGO hybrids. Int. J. Hydrogen Energy., 2023, 48, 27557-27567.

(10) S.-C. Sun, F.-X. Ma, H. Jiang, M.-X. Chen, P. Xu, L. Zhen, B. Song, C.-Y. Xu. Encapsulating dual-phase WC-W_2C nanoparticles into hollow carbon dodecahedrons for all-pH electrocatalytic hydrogen evolution. Chem. Eng. J., 2023, 462, 142132.

(11) T. Gong, J. Zhang, Y. Liu, L. Hou, J. Deng, C. Yuan. Construction of hetero-phase Mo_2C-CoO@N-CNFs film as a self-supported Bi-functional catalyst towards overall water splitting. Chem. Eng. J., 2023, 451, 139025.

(12) B. Yang, C. G. Wei, X. H. Wang, H. C. Fu, X. H. Chen, Q. Zhang, Y. H. Luo, H. Q. Luo, N. B. Li. Optimization of hydrogen adsorption on W_2C by late transition metaldoping for efficient hydrogen evolution catalysis. Materials Today Nano, 2023, 23, 100350.

(13) Y. Li, X. Wu, H. Zhang, J. Zhang. Interface Designing over WS_2/W_2C for

Enhanced Hydrogen Evolution Catalysis. ACS Appl. Energy Mater., 2018, 1, 3377-3384.

(14) Y. Hu, B. Yu, M. Ramadoss, W. Li, D. Yang, B. Wang, Y. Chen. Scalable Synthesis of Heterogeneous W-W_2C Nanoparticle-Embedded CNT Networks for Boosted Hydrogen Evolution Reactionin Both Acidic and Alkaline Media. ACS Sustainable Chem. Eng., 2019, 7, 11, 10016-10024.